Online ISSN 1848-3380, Print ISSN 0005-1144
ATKAFF 57(2), 361–371(2016)

Salem Saidi, Rabeh Abbassi, Nesrine Amor, Souad Chebbi

Passivity-Based Direct power control of Shunt Active Filter under Distorted Grid Voltage Conditions

DOI 10.7305/automatika.2016.10.1011
UDK 621.31.018.3.076-026.11:621.372.852.1-026.12

Original scientific paper

Despite its many advantages, the conventional direct power control (DPC) of shunt active power filters (SAPF) poses some problems. This paper investigates the design of a new control technical combining DPC control and passivity theory (PT) to ensure quasi-sinusoidal grid currents, under various conditions of the source voltages. The proposed approach (DPC-PT) appeals to the theory of symmetrical components (negative and positive) to solve the problem of disturbed voltages signals during a grid imbalance. The implantation of the DPC-PT methodology was developed under Matlab/Simulink environment. Simulation results showing the operation and performances of the SAPF in steady and transient states have been presented. The found results show the satisfactory dynamic response and the improvement of network behavior in the presence of an imbalance.

Key words: Direct power control, Passivity theory , Non-linear control, Fortescue theory, Power quality, Shunt active power filter, Unbalanced grid

Diretno upravljanje snagom aktivnog energetskog filtra u uvjetima asimetričnih faznih napona mreže zasnovano na pasivnosti. Unatoč brojnim prednostima, uz konvencionalni pristup direktnom upravljanju snage aktivnog energetskog filtra povezani su i određeni problemi. U ovom radu razmatra se sinteza novog pristupa upravljanju koji kombinira direktno upravljanje snagom i teoriju pasivnosti kako bi se osigurale kvazi-sinusoidalne struje mreže, u raznim uvjetima napona izvora. Predloženi pristup koristi teoriju simetričnih komponenti (negativna i pozitivna) za rješavanje problema poremećenih naponskih signala u uvjetima neravnoteža u mreži. Razvijena metoda upravljanja implementirana je u MATLAB/Simulink okruženju. Simulacijski rezultati pokazuju rad i učinkovitost predložene metode upravljanja u ustaljenom stanju i za vrijeme prijelaznih pojava. Rezultati pokazuju zadovoljavajuće tranzijente i poboljšanje vladanja mreže u uvjetima neravnoteža.

Ključne riječi: direktno upravljanje snagom, teorija pasivnosti, nelinearno upravljanje, Fortescueova teorija, kakvoća isporučene energije, aktivni energetski filtar, neravnoteže u mreži

1 INTRODUCTION

The progressive use of energy conversion systems, such as computer equipment, variable speed drives, power rectifiers in heavy industry and power of the oars subway via the overhead contact lines, significantly contributes to the degradation of the quality of electrical energy [1–3]. Indeed, these electrical equipment, absorbing non-sinusoidal currents, are harmonic generators leading disturbances in power grids [4, 5]. Thus, malfunction can occur in some electrical equipment that is overheating, the increasing of the harmonic distortion, the vibrations of rotating systems, noise and resonance phenomena, etc.

This situation resulted in the emergence of a growing concern to mitigate the emission of harmonics. Special attention has been brought to the passive filters. However, this type of devices, despite their wide use in industry, cause some problems i.e. the non adaptability to variations of the network and the load [4, 6]. In the same context, this situation has pushed researchers in power electronics and control to develop and to adjust advanced solutions, that are effective and able to overcome the disadvantages of the Passive filters. These solutions are known as active power filters [3, 7–9].

In the literature, several solutions of active filters have been proposed for the cleanup of the electrical networks [10, 11]. Currently, shunt active filters or series active filters as well as the combined series active and shunt passive power filters are those that best fulfils the constraints of energy production and distribution. In case where non linear loads are available among consumers, the harmonic currents are generated in the network. In these situations, the shunt active power filter (SAPF) is considered as the best solution for the mitigation of harmonics upstream of the polluter system and the compen-

sation of the reactive energy in applications of low and medium power so as to improve the effectiveness of the energy efficiency and power quality [12–14]. This type of filter allows to compensate for the disruptions even when the characteristics of the load change over time.

Since the advent of the SAPF, around about the 1882s, different control approaches have been proposed [15, 16]. All of these control strategies have been intended to achieve the same objectives, such as the joint improvement of the waveform of the different electrical quantities characterizing the electrical grid, the regulation of the DC link voltage and the reduction of its cost. Among these control approaches, two families can be identified, those who control the instantaneous currents and those who control the instantaneous active and reactive powers. These last are very interesting whenever it is necessary to ensure a direct and effective regulation of active and reactive power to their respective references.

The DPC is a control strategy that is simple, robust and easy to implement. It provides good performances in steady and transient states while ensuring a unity power factor with a decoupled control of active and reactive power. First, the idea of the DPC was to use the values of active and reactive powers as the main control variables instead of the instantaneous currents [6, 17, 18]. Generally the outer loop of the DPC is responsible for regulating the DC bus voltage to ensure the control of active power while operating at unit power factor is achieved by imposing reactive power to zero. The output of this loop is the input to the control inner loop that determines the control signals of the voltage source inverter either by using a switching table or using a space vector modulation (SVM). In classical control theory, linear models are considered. In order to determine the control laws in the presence of systems of non-linear differential equations, these systems, if they are linearizable, are close to a linear system control laws derived from such approach are sufficient in many practical applications, but in some cases the linear approach is not sufficient. Therefore, a theory for nonlinear control systems is necessary [10, 19–21]. In addition, most of the proposed approaches assume that the voltage source is balanced. However, any serious defect, which can not always be avoided, in any zone of the electrical network causes a difference in amplitude of rms voltage and / or phase problems. In these circumstances, this imbalance leads to the appearance of the harmful negative sequence.

In this context, this paper proposes a new control technique of a SAPF to compensate harmonic distortion caused by nonlinear load when the source voltages are unbalanced and/or distorted. The developed technique is based on the combination of DPC theory with passive control with a nonlinear controller having more robustness. In the proposed approach, the method of resolution of unbalanced three-phase systems is based on Fortescue theory that deals with complex quantities in real and imaginary parts. Fortescue theory is based on the idea that any unbalanced, voltages and / or currents, system can be broken down into three balanced sub-systems namely the direct system (positive sequence), the inverse system (negative sequence) and the zero-sequence system (zero sequence).

2 SYSTEM DESCRIPTION

The purpose of using the proposed structure (Fig. 1) is to clean up the harmonic current consumed by the load and to compensate of the reactive energy. The active filter acts as a controlled current source which acts on the grid current in order to improve its characteristics in terms of harmonics distortion.

For proper functioning of the set (SAPF, grid and load), a power balance between the power supplied by the source, that of the parallel active filter and the instantaneous power consumed by the nonlinear load is established. If $p_g(t)$ and $q_g(t)$ are the active and reactive powers supplied by the distribution network, $p_f(t)$ and $q_f(t)$ are the active and reactive instantaneous powers provided by the SAPF respectively, so to compensate reactive power and eliminate the harmonic currents, the distribution network must provide:

$$\begin{cases} p_g(t) = \overline{p}_l(t), \\ q_g(t) = 0. \end{cases} \tag{1}$$

Moreover, the oscillatory component $p_l(t)$ must be provided by the SAPF and the grid, while the amount of the reactive power absorbed by the load shall be provided in its entirety by the SAPF:

$$\begin{cases} p_f(t) = p_l(t) - p_g(t) = \tilde{p}_l(t), \\ q_f(t) = q_l(t) - q_g(t) = q_l(t). \end{cases} \tag{2}$$

The equations (1) and (2) govern the power flow between the pollutant load, the electrical network and the active power filter during transitional regimes following an adverse impact or a load shedding. This power is reflected in a change in the voltage across the DC-bus capacitor. For this reason, it is necessary to apply a control of the DC bus voltage to control its level in the steady state and limiting its fluctuations transients in transitional arrangements.

3 PROPOSED CONTROL TECHNIQUE

The main purpose of the control strategy is to get, on the one hand, a rapid response of active and reactive powers to reach their desired values respectively $p_g^*(t)$ and $q_g^*(t)$, i.e. if $p_g(t) \longmapsto p_g^*(t)$ and $q_g(t) \longmapsto q_g^*(t)$ if $t \longmapsto \infty$. On the other hand, the objective is to

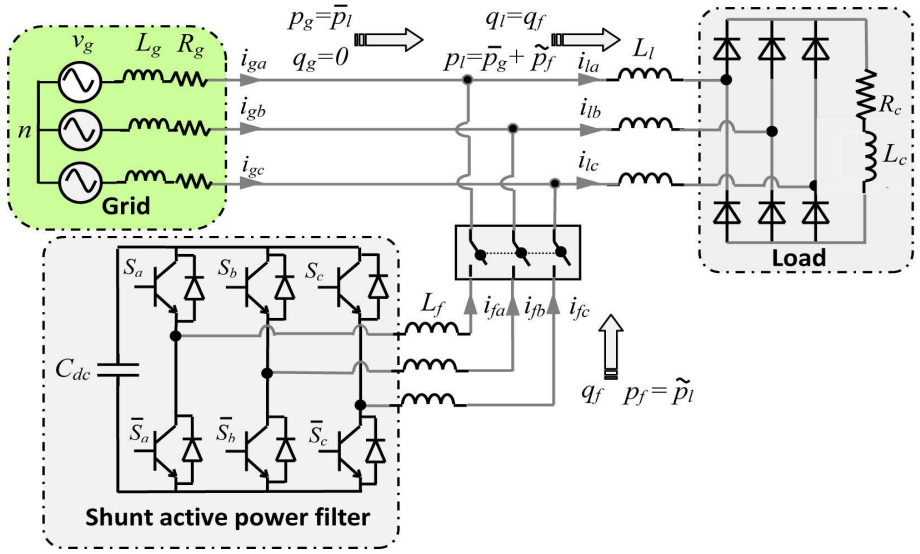

Fig. 1. Schematic diagram of the SAPF model

maintain the DC bus voltage close to its reference value $v_{dc}(t) \longmapsto v^*_{dc}(t)$.

In addition, it can be noted that the reactive power reference is fixed null ($q^*_g(t) = 0$) to ensure operating at unit power factor while active power reference is obtained from the DC bus voltage regulator.

3.1 Voltage description in the unbalanced case

For each phase the fundamental voltages and the harmonic voltages are written, separately, as follows:

$$\mathbf{v}_{g\alpha\beta}(t) = \mathbf{v}_{g\alpha\beta,f}(t) + \mathbf{v}_{g\alpha\beta,h}(t). \tag{3}$$

The Fortescue theory is applied to the voltages system (3). The new voltages, depending on the positive and negative sequences, are obtained as follows:

$$\mathbf{v}_{g\alpha\beta}(t) = \mathbf{v}^p_{g\alpha\beta,f}(t)+\mathbf{v}^n_{g\alpha\beta,f}(t)+\mathbf{v}^p_{g\alpha\beta,h}(t)+\mathbf{v}^n_{g\alpha\beta,h}(t). \tag{4}$$

These voltages can be divided as (5):

$$\begin{aligned}\mathbf{v}_{g\alpha\beta}(t) = {} & e^{\mathbf{J}\omega t}\mathbf{V}^p_{g\alpha\beta,f}(t) + e^{-\mathbf{J}\omega t}\mathbf{V}^n_{g\alpha\beta,f}(t) \\ & + \sum_{k\in\mathcal{H}} e^{\mathbf{J}k\omega t}\mathbf{v}^p_{g\alpha\beta,h}(t) + \sum_{k\in\mathcal{H}} e^{\mathbf{J}k\omega t}\mathbf{v}^n_{g\alpha\beta,h}(t).\end{aligned} \tag{5}$$

Herein, $\mathbf{v}^p_{g\alpha\beta,f}(t)$ and $\mathbf{v}^n_{g\alpha\beta,f}(t)$ are, respectively, the positive and negative sequences of the distribution grid voltages system at the fundamental frequency $\alpha\beta$, $\mathbf{v}^p_{g\alpha\beta,h}(t)$ and $\mathbf{v}^n_{g\alpha\beta,h}(t)$ are respectively the positive and negative sequences of the harmonic voltages, ω is the grid fundamental angular frequency, $\mathbf{V}^p_{g\alpha\beta,h}(t)$ and $\mathbf{V}^n_{g\alpha\beta,h}(t)$ are the components related to various direct and quadrature harmonic components of the positive and negative sequences of the grid voltages, $\mathbf{V}^p_{g\alpha\beta,f}(t)$ and $\mathbf{V}^n_{g\alpha\beta,f}(t)$ are the components related to direct and quadrature fundamental components of the positive and negative sequences of the grid voltages, $k \in \mathcal{H} = \{5, 7, 11, ...\}$ is the harmonic order and The operator $e^{\mathbf{J}\omega t}$ presents the rotation matrix defined by:

$$e^{\mathbf{J}\omega t} = \begin{bmatrix} cos(\omega t) & -sin(\omega t) \\ sin(\omega t) & cos(\omega t) \end{bmatrix}, \tag{6}$$

where

$$\mathbf{J} = \begin{bmatrix} 0 & -1 \\ 1 & 0 \end{bmatrix}.$$

In addition, we recall that the SAPF allows, when an appropriate control strategy is applied, to compensate all power disturbances when the nonlinear load is subjected to a sinusoidal voltage. Thus, the two voltages from equation (5) are written as follows:

$$\begin{aligned}\mathbf{v}_{g\alpha\beta}(t) &= e^{\mathbf{J}\omega t}\mathbf{V}^p_{g\alpha\beta,f}(t) + e^{-\mathbf{J}\omega t}\mathbf{V}^n_{g\alpha\beta,f}(t), \\ &= \mathbf{v}_{g\alpha\beta,f}(t) + \mathbf{v}_{g\alpha\beta,h}(t).\end{aligned} \tag{7}$$

From (7), the source voltages, under unbalanced state, are expressed by the following relationships:

$$\dot{\mathbf{v}}_{g\alpha\beta}(t) = \mathbf{J}\omega\phi_{g\alpha\beta}(t), \tag{8}$$

$$\dot{\phi}_{g\alpha\beta}(t) = \mathbf{J}\omega\mathbf{v}_{g\alpha\beta}(t). \tag{9}$$

It should be noted that the use of the auxiliary variable $\phi_{g\alpha\beta}(t) = \mathbf{v}^p_{g\alpha\beta}(t) - \mathbf{v}^n_{g\alpha\beta}(t)$ allows a complete description of the grid voltages imbalance. In balanced case, the voltages system of the source is expressed by $\dot{\mathbf{v}}_{g\alpha\beta}(t) = \mathbf{J}\omega\mathbf{v}_{g\alpha\beta}(t)$.

3.2 PQ theory in the unbalanced case

The grid powers are expressed as:

$$\begin{bmatrix} p_g(t) \\ q_g(t) \end{bmatrix} = \begin{bmatrix} v_{g\alpha}(t) & v_{g\beta}(t) \\ -v_{g\beta}(t) & v_{g\alpha}(t) \end{bmatrix} \begin{bmatrix} i_{g\alpha}(t) \\ i_{g\beta}(t) \end{bmatrix} = \mathcal{C}(t)\mathbf{i}_{g\alpha\beta}(t). \tag{10}$$

From equation (10), the current vector is deduced as:

$$\mathbf{i}_{g\alpha\beta}(t) = \mathcal{C}^{-1}(t) \begin{bmatrix} p_g(t) \\ q_g(t) \end{bmatrix}. \tag{11}$$

The derivation of the above expression gives:

$$\dot{\mathbf{i}}_{g\alpha\beta}(t) = \dot{\mathcal{C}}^{-1}(t) \begin{bmatrix} p_g(t) \\ q_g(t) \end{bmatrix} + \mathcal{C}^{-1}(t) \begin{bmatrix} \dot{p}_g(t) \\ \dot{q}_g(t) \end{bmatrix}. \tag{12}$$

Taking into account (10), (9) and (8), the relation (12) can be rewritten as follows:

$$\dot{\mathbf{i}}_{g\alpha\beta}(t) = \mathbf{J}\omega \begin{bmatrix} \delta(t) \\ \gamma(t) \end{bmatrix} + \mathcal{C}^{-1}(t) \begin{bmatrix} \dot{p}_g(t) \\ \dot{q}_g(t) \end{bmatrix}. \tag{13}$$

Herein:

$$\begin{aligned} \begin{bmatrix} \delta(t) \\ \psi(t) \end{bmatrix} &= \begin{bmatrix} \phi_{g\alpha}(t) & \phi_{g\beta}(t) \\ -\phi_{g\beta}(t) & \phi_{g\alpha}(t) \end{bmatrix} \begin{bmatrix} i_{g\alpha}(t) \\ i_{g\beta}(t) \end{bmatrix} \\ &= \mathcal{R}^{-1}(t)\mathcal{C}^{-1}(t) \begin{bmatrix} p_g(t) \\ q_g(t) \end{bmatrix}. \end{aligned} \tag{14}$$

In general, it is assumed that the resistance R_g is negligible [10]. This allows for:

$$L\frac{d\mathbf{i}_{g\alpha\beta}(t)}{dt} = -\mathbf{v}_{f\alpha\beta}(t) + \mathbf{v}_{g\alpha\beta}(t). \tag{15}$$

Taking into account (13) and (15), we deduce:

$$\begin{bmatrix} L\dot{p}_g(t) \\ L\dot{q}_g(t) \end{bmatrix} = \mathcal{C}(t)(-\mathbf{v}_{f\alpha\beta}(t) + \mathbf{v}_{g\alpha\beta}(t)) - \sigma\mathbf{J} \begin{bmatrix} \delta(t) \\ \psi(t) \end{bmatrix}, \tag{16}$$

with $\sigma = \omega L$.

3.3 Passivity based DPC

In general, the design of a passivity-based control (PBC) emulates the system while increasing the rate of convergence of the state to the point of equilibrium with the modeling of energy and the damping injection. This procedure involves making a copy of the system around the desired reference values to which certain damping terms are included as follows:

$$\begin{aligned} \begin{bmatrix} L\dot{p}_g^*(t) \\ L\dot{q}_g^*(t) \end{bmatrix} &= \mathcal{C}(t)\left(-\mathbf{v}_{f\alpha\beta}(t) + \mathbf{v}_{g\alpha\beta}(t)\right) \\ &\quad - \hat{\sigma}\mathbf{J} \begin{bmatrix} \delta(t) \\ \psi(t) \end{bmatrix} + \mathcal{D}^k \begin{bmatrix} \tilde{p}_g(t) \\ \tilde{q}_g(t) \end{bmatrix}, \end{aligned} \tag{17}$$

where $\hat{\sigma}$ represents the estimation of σ, $\mathcal{D}^k = diag\{k_p, k_q\}$ which is the damping injection matrix, k_p and k_q are positive damping injection values for $p_g(t)$ and $q_g(t)$ powers, respectively. and $\tilde{p}_g(t) = p_g(t) - p_g^*(t)$ and $\tilde{q}_g(t) = q_g(t) - q_g^*(t)$ are the regulation errors.

Considering that the instructions are kept constant, i.e. $[\dot{p}_g^*(t)\ \dot{p}_g^*(t)] = [0\ 0]$, the solving of the above equation allows to express the control vector as follows

$$\begin{aligned} \mathbf{v}_{f\alpha\beta}(t) &= \mathbf{v}_{g\alpha\beta}(t) + \mathcal{C}^{-1}(t) \\ &\quad .\left\{ -\hat{\sigma}\mathbf{J} \begin{bmatrix} \delta(t) \\ \psi(t) \end{bmatrix} + \mathcal{D}^k \begin{bmatrix} \tilde{p}_g(t) \\ \tilde{q}_g(t) \end{bmatrix} \right\}. \end{aligned} \tag{18}$$

From the closed loop system (16) and the control vector (18), the error model is obtained as:

$$\begin{bmatrix} L\dot{\tilde{p}}_g(t) \\ L\dot{\tilde{q}}_g(t) \end{bmatrix} = -\mathcal{D}^k \begin{bmatrix} \tilde{p}_g(t) \\ \tilde{q}_g(t) \end{bmatrix} + \tilde{\sigma}\mathbf{J} \begin{bmatrix} \delta(t) \\ \psi(t) \end{bmatrix}, \tag{19}$$

where $\tilde{\sigma} = \sigma - \hat{\sigma}$.

Since the feature of this error model follows the approach of Lyapunov, the total energy of a system error, denoted $\mathcal{X}(t)$, is:

$$\mathcal{X}(t) = \frac{L}{2}\tilde{p}_g^2(t) + \frac{L}{2}\tilde{q}_g^2(t) + \frac{1}{2\gamma}\tilde{\sigma}^2(t). \tag{20}$$

Its derivative with respect to time is expressed as follows:

$$\dot{\mathcal{X}}(t) = L\dot{\tilde{p}}_g(t)\tilde{p}_g(t) + L\dot{\tilde{q}}_g(t)\tilde{q}_g(t) + \frac{1}{\lambda}\dot{\tilde{\sigma}}(t)\tilde{\sigma}(t). \tag{21}$$

By using the error model (19), the equation (21) can be expressed as:

$$\begin{aligned} \dot{\mathcal{X}}(t) &= -k_p\tilde{p}_g^2(t) - k_q\tilde{q}_g^2(t) + \frac{1}{\lambda}\dot{\tilde{\sigma}}(t)\tilde{\sigma}(t) \\ &\quad + \tilde{\sigma}(t) \begin{bmatrix} \tilde{p}_g(t) & \tilde{p}_g(t) \end{bmatrix} \mathbf{J} \begin{bmatrix} \delta(t) \\ \psi(t) \end{bmatrix}. \end{aligned} \tag{22}$$

In order to ensure Lyapunov stability, we propose that:

$$\begin{aligned} \dot{\tilde{\sigma}}(t) &= -\lambda \begin{bmatrix} \tilde{p}_g(t) & \tilde{p}_g(t) \end{bmatrix} \mathbf{J} \begin{bmatrix} \delta(t) \\ \psi(t) \end{bmatrix} \\ &= -\lambda\left(\tilde{p}_g(t)\gamma(t) - \tilde{p}_g(t)\delta(t)\right), \end{aligned} \tag{23}$$

where λ is a positive constant.

In the same context, if we consider that σ is constant and satisfying the property $\dot{\tilde{\sigma}}(t) = \dot{\hat{\sigma}}(t)$, the expression described in (20) becomes:

$$\dot{\mathcal{X}}(t) = -k_p\tilde{p}_g^2(t) - k_q\tilde{q}_g^2(t). \tag{24}$$

For the reasons raised, some researchers have replaced the sensors by estimators based on static and dynamic equations of SAPF.

3.4 Estimation of the auxiliary variable

In many applications, the measurement of the entire state is not possible. This is due to reliability constraints or even economic. So, it is necessary to reconstruct the variables unmeasured state using the available measures. In the same context, an estimator is used to estimate the auxiliary variable $\phi_{g\alpha\beta}(t)$ using measurements of voltages. The general idea of the proposed estimator is composed of a copy of the model equations, already established (8) and (9), in which a damping term is added. The expression of the estimator obtained in this case is:

$$\dot{\hat{\mathbf{v}}}_{g\alpha\beta}(t) = \mathbf{J}\omega\dot{\hat{\phi}}_{g\alpha\beta}(t) + \gamma\tilde{\mathbf{v}}_{g\alpha\beta}(t), \tag{25}$$

$$\dot{\hat{\phi}}_{g\alpha\beta}(t) = \mathbf{J}\omega\hat{\mathbf{v}}_{g\alpha\beta}(t), \tag{26}$$

where $\tilde{\mathbf{v}}_{g\alpha\beta}(t) = \mathbf{v}_{g\alpha\beta}(t) - \hat{\mathbf{v}}_{g\alpha\beta}(t)$ is the error between the actual status and the estimated state, $\hat{\mathbf{v}}_{g\alpha\beta}(t)$ and $\hat{\phi}_{g\alpha\beta}(t)$ are the observed quantities of $\mathbf{v}_{g\alpha\beta}(t)$ and $\phi_{g\alpha\beta}(t)$ and γ is the estimator gain.

The dynamic error of the estimator is given with:

$$\dot{\tilde{\mathbf{v}}}_{g\alpha\beta}(t) = \mathbf{J}\omega\dot{\tilde{\phi}}_{g\alpha\beta}(t) - \gamma\tilde{\mathbf{v}}_{g\alpha\beta}(t), \tag{27}$$

$$\dot{\tilde{\phi}}_{g\alpha\beta}(t) = \mathbf{J}\omega\tilde{\mathbf{v}}_{g\alpha\beta}(t). \tag{28}$$

Herein, $\tilde{\phi}_{g\alpha\beta}(t) = \phi_{g\alpha\beta}(t) - \hat{\phi}_{g\alpha\beta}(t)$ is the error of the auxiliary variable.

In addition, we can conclude that the estimator obtained is entirely consistent with the Lyapunov candidate function. In this condition, we succeeded to express the function of the squared error by:

$$\mathcal{W}(t) = \frac{1}{2}\tilde{\mathbf{v}}^2_{g\alpha\beta}(t) + \frac{1}{2}\tilde{\phi}^2_{g\alpha\beta}(t). \tag{29}$$

Its derivative with respect to time along the trajectory is:

$$\dot{\mathcal{W}}(t) = \tilde{\mathbf{v}}^T_{g\alpha\beta}(t)\dot{\tilde{\mathbf{v}}}_{g\alpha\beta}(t) + \tilde{\phi}^T_{g\alpha\beta}(t)\dot{\tilde{\phi}}_{g\alpha\beta}(t). \tag{30}$$

Taking into account the error model of the two equations (27) and (28) we deduce the expression of the derivative of the energy:

$$\dot{\mathcal{W}}(t) = -\gamma\tilde{\mathbf{v}}^T_{g\alpha\beta}(t)\dot{\tilde{\mathbf{v}}}_{g\alpha\beta}(t). \tag{31}$$

$\mathcal{W}(t)$ is a defined positive quadratic function and $\dot{\mathcal{W}}(t)$ is a negative semi defined function which involves the origin of the stability of the system error in the sense of Lyapunov.

3.5 Anti-Windup PI control of Capacitor Voltage

Knowing that the energy storage of the DC side is provided by the capacitor(C_{dc}), regulation of the DC bus voltage is of paramount importance. For this reason, a proportional integral (PI) corrector is used, in our algorithm, to maintain constant voltage DC bus, to limit fluctuations in the supply voltage of the SAPF filter and to prohibit the deterioration of filtering performance.

After processing the difference between the measured value ($v_{dc}(t)$) and its reference value ($v^*_{dc}(t)$), the output of the control loop provides an estimation of the maximum current of the source $I_{sm}(t)$. This current is used to calculate the reference power ($p^*_g(t)$) requested by the filter and the losses caused by the switches of the converter.

Under normal operation, significant variations in the set size can cause saturation phenomena of internal quantities. These phenomena, comparable to nonlinearities degrade the dynamic behavior of the system if they are not properly controlled. The proposed solution is to introduce a fictive gap ($\varepsilon_f(t) = I_{sm}(t) - I_{smf}(t)$))) in the input of the integrator when the control member deviates from its trajectory. Therefore, the controller output is expressed by:

$$\begin{cases} I_{sm}(t) = k_p\varepsilon(t) + k_i\displaystyle\int\varepsilon(t)\,\mathrm{d}t, \\ I_{sm}(t) = k_p\varepsilon(t) + k_i\displaystyle\int\left(\varepsilon(t) - \frac{1}{\tau_i}\varepsilon_f(t)\right)\mathrm{d}t. \end{cases} \tag{32}$$

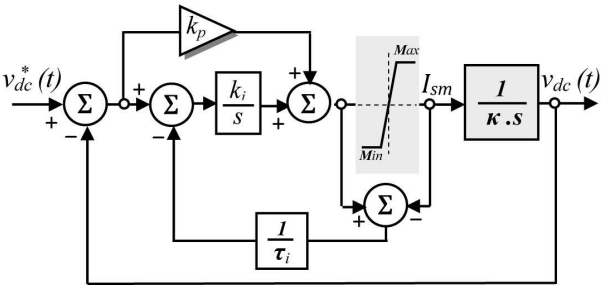

Fig. 2. Control closed loop of DC voltage

It should be noted that the current $I_{sm}(t)$ is obtained by applying the controller transfer function of the DC bus voltage $G_{PI}(p)$ to the instantaneous $\varepsilon(t)$ between the reference of the DC link voltage and its measured value across the capacitor C_{dc} (Fig.2). In these conditions, the current $I_{sm}(t)$ is given by:

$$I_{sm}(t) = G_{PI}(p)\left(v^*_{dc}(t) - v_{dc}(t)\right). \tag{33}$$

From the block diagram of the Fig. 2, the closed-loop transfer function of the system can be written:

$$\frac{v_{dc}(p)}{v^*_{dc}(p)} = \frac{k_p.s + k_i}{\boldsymbol{\kappa}.s^2 + k_p.s + k_i} = \frac{\frac{k_p}{\boldsymbol{\kappa}}(s + \frac{k_i}{k_p})}{s^2 + \frac{k_p}{\boldsymbol{\kappa}} + \frac{k_i}{\boldsymbol{\kappa}}}, \tag{34}$$

where:

$$\boldsymbol{\kappa} = \frac{\sqrt{2}C_{dc}v^*_{dc}}{3V_s}.$$

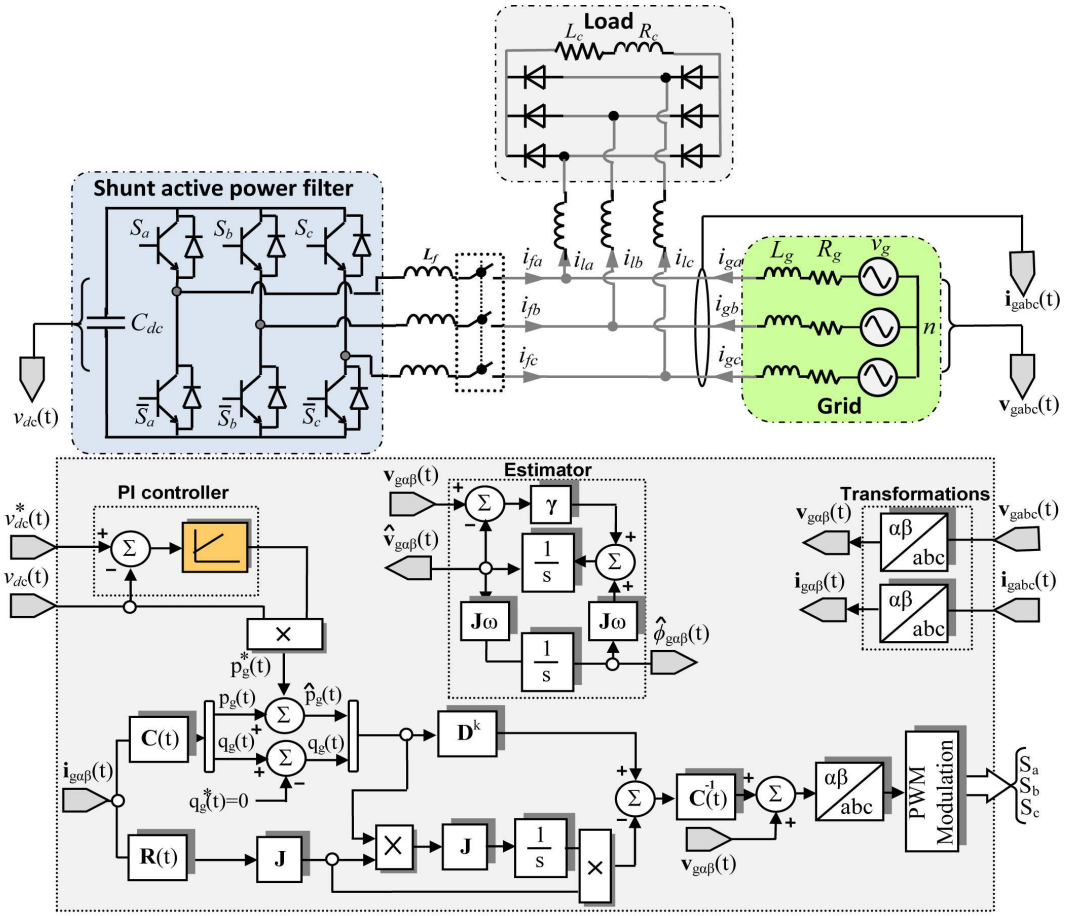

Fig. 3. Block diagram of the passivity based direct power control

From the last equation, the coefficients ki and kp are identified as follows:

$$\begin{cases} ki = \kappa\omega_c^2, \\ kp = 2\xi\omega_c\kappa, \end{cases} \tag{35}$$

where ω_c and ξ are the cutoff angular frequency and the damping factor, respectively.

After the theoretical study of the control strategy described above, the functional model on Matlab environment using Simulink blocks and SymPowerSystems library ha been developed in order to validate the functionality of the proposed strategy.

4 SIMULATION RESULTS AND DISCUSSION

After having exposed the models of the proposed control strategy, the present section reveals the simulations results. The goal is to validate the functionality of the proposed strategy in order to compensate the reactive power and to eliminate the harmonic pollution under different operating conditions of the source. The characteristics of the source, the pollutant load and those of the SAPF filter are detailed in the Tab. 1. The models of the power section, especially the pollutant load, the inverter, the electrical grid and the filter output have been built using Toolbox Power System.

Table 1. Parameters of the analysed system

Quantity	Symbol	Value
Grid voltage L-N	Vs	230 V
Grid frequency	f_g	50 Hz
Grid resistance	R_g	0.02 Ω
Grid inductance	L_g	200 μH
Filter resistance	R_f	0.05 Ω
Filter inductance	L_f	1.35 mH
SAPF DC capacitor	c_{dc}	1600 μF
DC link capacitor	v_{dc}^*	565 V
AC Line resistance	R_l	0.05 Ω
AC Line inductance	L_l	3 mH
DC Load resistance	R_c	9 or 13 Ω
DC Load inductance	L_c	25 mH

4.1 Grid-connected SAPF filter

In the presence of a nonlinear load emulated by a three phase full wave bridge rectifier connected to a three phase network, the grid behavior, after the insertion of the SAPF at time $t = 0.1s$, has been simulated. The simulation results obtained with the proposed control strategy are shown in Figures 4, 5 and 6. The wave forms of the powers, the currents of the source and also the spectral analysis of the source currents. It is observed that after the integration of the SAPF, the harmonic component of active power $(p_g(t))$ and the reactive power of the source $(q_g(t))$ are zero; this confirms the unity power factor (Fig.4).

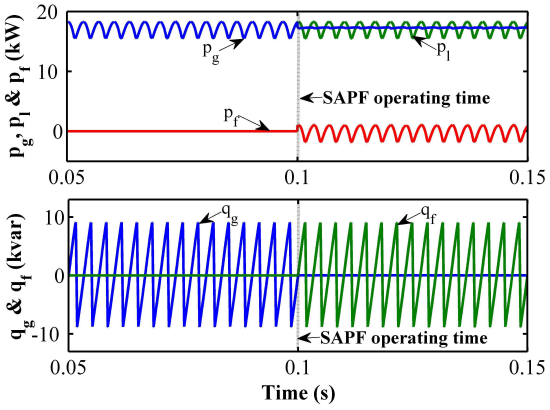

Fig. 4. Active and Reactive power sharing between load, grid and SAPF

In addition the results show a significant improvement in the waveform of the grid current (Fig. 5). This current has been de-polluted at a satisfactory level. Furthermore, there is an improvement of the power factor (PF) insofar as the current $i_{ga}(t)$ and the voltage $v_{ga}(t)$ are perfectly in phase (Fig. 6 and Fig. 7). On the basis that the current $i_{ga}(t)$ reached to recover its sinusoidal form, it can be confirmed that the SAPF filter achieves to generate an harmonic current $i_{fa}(t)$ having the same amplitude but in opposition of phase with that absorbed by the nonlinear load (Fig. 5). The THD of the grid side currents is reduced to 0.82% while it was 36.05% before compensation (Tab.2).

Table 2. THD of the grid currents

Grid currents	Before connection	After connection
$i_{ga}(t)$	0.82%	28.05%
$i_{gb}(t)$	0.84%	27.01%
$i_{gc}(t)$	0.8%	28.50%

Similarly, it is proved that the DC bus voltage $(v_{dc}(t))$ is properly regulated to its reference value imposed by the proposed control with good stability and accuracy (Fig. 7).

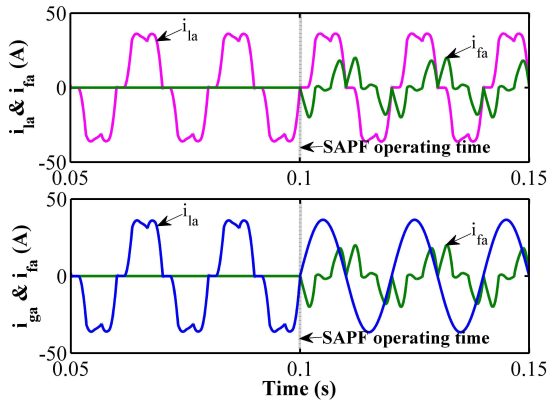

Fig. 5. Load, grid and SAPF currents before and after connection of SAPF to the grid

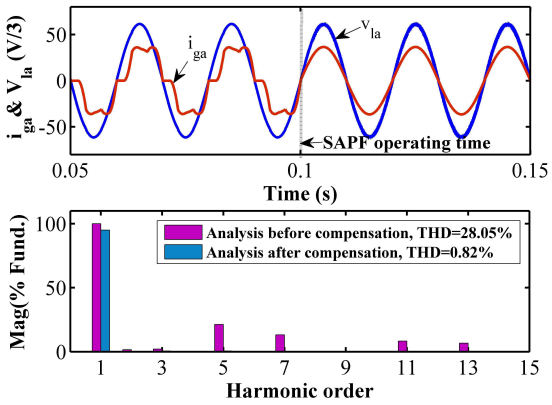

Fig. 6. Load voltage, grid current and harmonic analysis

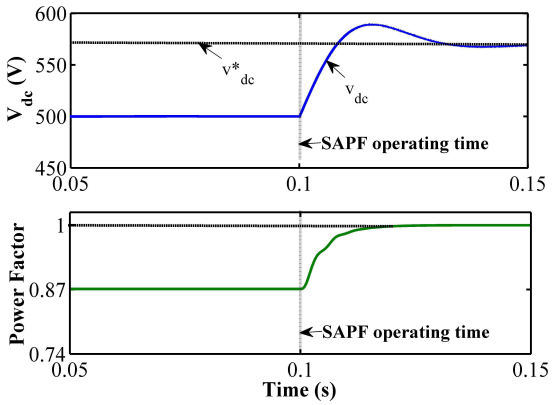

Fig. 7. DC-Link voltage and PF of grid, before and after connection of SAPF to the grid

As a conclusion, it can be confirmed that the results of the integration of SAPF filter is satisfactory, in steady state.

4.2 Dynamic performance of

In order to study the performances and the behavior of the SAPF during a transitional regime due to the presence of a pollutant load, it has been assumed that a reduction of about 30% of the load resistance occurred at time $t = 0.2$ s. Based on the waveforms of the load current, the source current and the filter current in the phase "a" (Fig. 8 and Fig. 10), we confirm the good dynamic response of the proposed control strategy. It has been shown that the load resistance reduction will result in a change in the absorbed current (Fig. 8) and accordingly a reduction of the current injected by the filter as well as reference of the instantaneous active power supplied by the controller PI (Fig. 9). Indeed, the current network amounts to its new amplitude, instantaneously ($is = 46$ A) keeping its sinusoidal shape. The DC bus voltage drops of $\Delta v_{dc} = 20$ V, due to this power demand, and undergoes a transient before joining its reference $\Delta t = 75$ ms. Furthermore, we note that the reactive power has not been affected during this variation of the load. Indeed, it is continuing its null reference to ensure proper reactive power compensation control and the regulation model keeps precisely the active power to its new value requested by the nonlinear load (Fig. 9). Similarly, we note that an acceptable overshoot (2%) in the active power magnitude has arisen since the change in nonlinear load. These results show that the used PI controller offers excellent performances, not only in pursuit but also in control, with a very good tracking of the DC bus voltage reference during the load change (Fig. 10). When the load current is increased, capacitor voltage decreases (increases) to compensate for the real power supplied by the source.

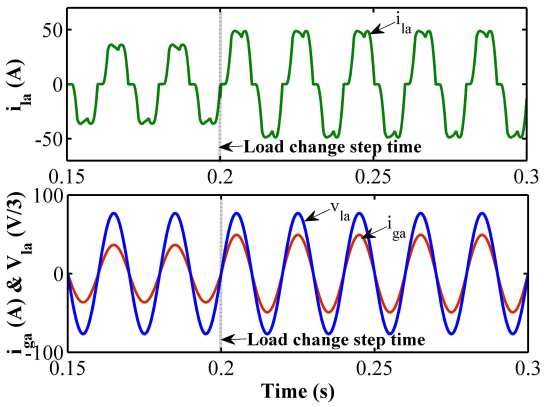

Fig. 8. Load current, load voltage and grid current, step load change

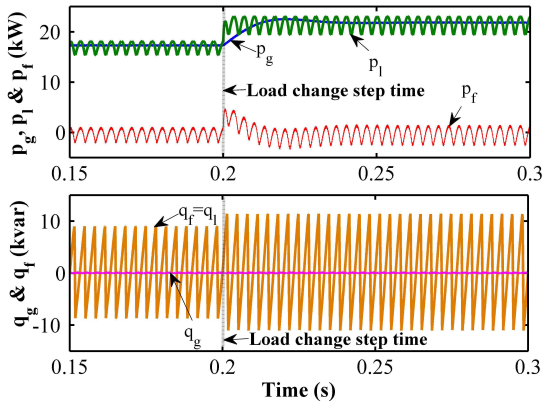

Fig. 9. Active and reactive powers (source,filter and load), step load change

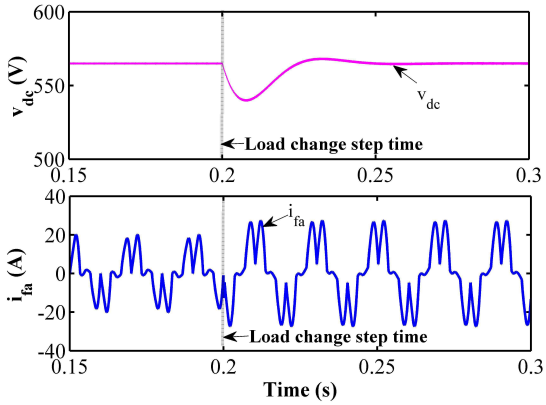

Fig. 10. DC-Link voltage and filter current, step load change

After having stated these figures in case of a load variation, we confirm satisfactory dynamics of the proposed strategy. This does has not prevented us to consider another fault scenario that involves a grid imbalance

4.3 Case of unbalanced voltage System

In order to quantify the contribution of the proposed control strategy, a scenario that involves an imbalance of voltage source has been simulated. The rms values of phase voltages « a » «b » and « c » are 230 V, 276 V and 184 V, respectively.

In the presence of the fault mentioned above, the temporal evolution of source voltages (Fig. 11) and the grid currents have been depicted (Fig. 12). Based on the observed characteristics, it was found that the proposed control can take into account the grid imbalances since that the SAPF provides harmonic current allowing to get sinusoidal

and balanced currents (Fig. 13 and Fig. 14). Particularly, there is no phase change or unacceptable amplitude overshoot. This can be seen through the current and the voltage of the source before and after the compensation. According to the observed behavior, it should be noted that the influence of a such voltage unbalance is negligible. All of these performances confirm the potential of the developed control strategy. In order to assess the robustness and to highlight the improvement of DPC by the use of the passivity theory, some simulations consisting on the variation of $v^*_{dc(t)}$ and C for a fixed charge have been made. Under these conditions, it can be noticed that the THD of the resulting current is eligible over all the variation range (Fig. 15).

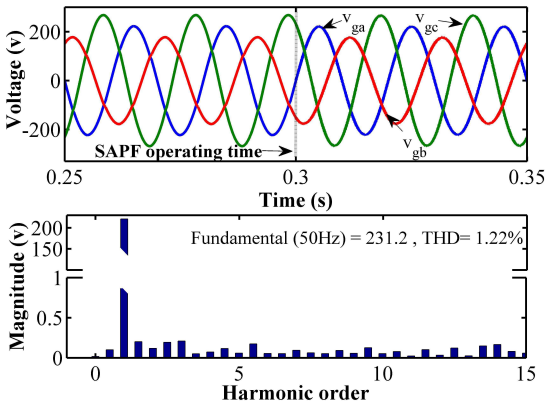

Fig. 11. Three-phase source voltages and frequency spectrum of source voltage of phase-a

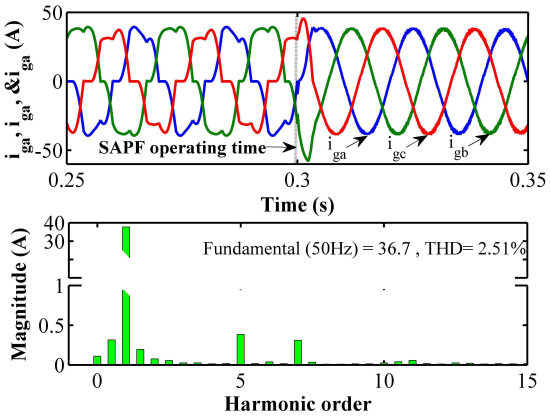

Fig. 12. Three-phase source currents and frequency spectrum of source current of phase-a

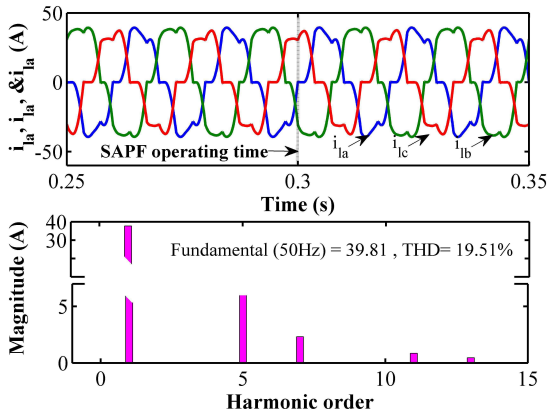

Fig. 13. Three-phase load currents and frequency spectrum of load current of phase-a

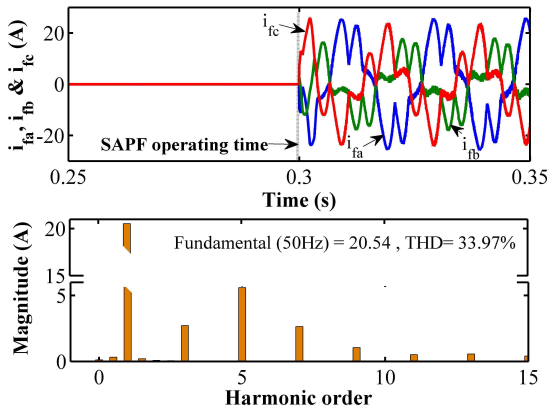

Fig. 14. Three-phase compensator currents and frequency spectrum of compensator current of phase-a

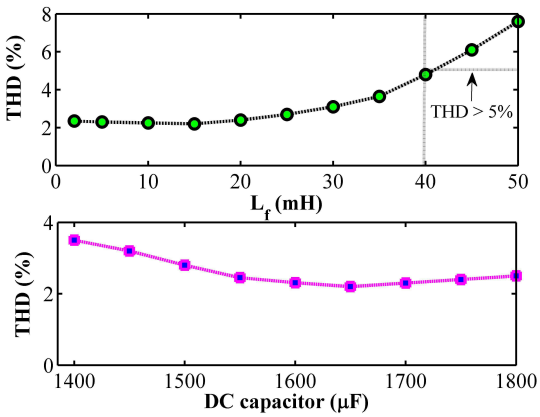

Fig. 15. Simulation results of robustness examination

5 CONCLUSION

This paper presents a new configuration of the direct control of power, applied to the SAPF, which aptly fits with unbalanced states of the electrical grid. The proposed control strategy, based on the passive control, has contributed to the improvement of the power quality of the electric energy in distribution networks. The choice of passive control has been justified since it is known as an efficient tool able to control the complex and highly nonlinear systems. This strategy, which is based upon the theory of Fortescue, has led to a better source current in steady state, following a sudden change of the nonlinear load and during grid imbalance. The results obtained by this approach have confirmed its good performances while carrying out the desired compensation during severe voltage disturbances.

REFERENCES

[1] H. Akagi, Y. Kanazawa, and A. Nabae, "Instantaneous reactive power compensators comprising switching devices without energy storage components," *IEEE Transactions On Industry Applications*, vol. 20, no. 3, pp. 625–630, 1984.

[2] A. Bhattacharya, C. Chakraborty, and S. Bhattacharya, "Parallel connected shunt hybrid active power filters operating at different switching frequencies for improved performance," *IEEE Transactions On Industrial Electronics*, vol. 59, no. 11, pp. 4007–4019, 2012.

[3] S. Saidi, R. Abbassi, and S. Chebbi, "Virtual flux based direct power control of shunt active filter," *Scientia Iranica Transactions D: Computer Science & Engineering and Electrical Engineering*, vol. 26, no. 6, pp. 2165–2176, 2014.

[4] H. Kim, F. Blaabjerg, B. Bak-Jensen, and J. Choi, "Instantaneous power compensation in three-phase systems by using p–q–r theory," *IEEE Transactions On Power Electronics*, vol. 17, no. 5, pp. 701–710, 2002.

[5] S. P. Litran and P. Salmeron, "Analysis and design of different control strategies of hybrid active power filter based on the state model," *IET Power Electronics*, vol. 5, no. 8, pp. 1341–1350, 2012.

[6] R. Mahanty, "Indirect current controlled shunt active power filter for power quality improvement," *Electrical Power and Energy Systems*, vol. 62, no. 2, pp. 441–449, 2014.

[7] L. Shang, D. Sun, and J. Hu, "Control analysis of an active power filter using lyapunov candidate," *IET Power Electronics*, vol. 2, no. 4, pp. 325–334, 2008.

[8] R. Abbassi and S. Chebbi, "Energy management strategy for a grid–connected wind-solar hybrid system with battery storage: policy for optimizing conventional energy generation," *International Review of Electrical Engineering*, vol. 7, no. 2, pp. 979–3990, 2012.

[9] P. Dey and S. Mekhilef, "Current controllers of active power filter for power quality improvement: A technical analysis," *Automatika*, vol. 56, no. 1, pp. 42–54, 2015.

[10] L. Shang, D. Sun, and J. Hu, "Sliding-mode-based direct power control of grid-connected voltage-sourced inverters under unbalanced network conditions," *IET Power Electronics*, vol. 4, no. 5, pp. 570–579, 2011.

[11] S. Rahmani, A. Hamadi, and K. Al-Haddad, "Lyapunov-function-based control for a three-phase shunt hybrid active filter," *IEEE Transactions On Industrial Electronics*, vol. 59, no. 3, pp. 1418–1429, 2012.

[12] H. Komurcugil and O. Kukrer, "New control strategy for single-phase shunt active power filters using a lyapunov function," *IEEE Transactions On Industrial Electronics*, vol. 53, no. 1, pp. 305–312, 2006.

[13] W.-H. Choi, C.-S. Lam, M.-C. Wong, and Y.-D. Han, "Analysis of dc-link voltage controls in three-phase four-wire hybrid active power filters," *IEEE Transactions On Power Electronics*, vol. 28, no. 5, pp. 2180– 2191, 2013.

[14] S. Saidi, R. Abbassi, and S. Chebbi, "Fuzzy logic controller for three-level shunt active filter compensating harmonics and reactive power," *International Journal of Adaptive Control and Signal Processing*, vol. 30, no. 6, pp. 809–823, 2016.

[15] S. Rahmani, A. Hamadi, K. Al-Haddad, and L. A. Dessaint, "A combination of shunt hybrid power filter and thyristor-controlled reactor for power quality," *IEEE Transactions on Industrial Electronics*, vol. 61, no. 5, pp. 2152–2164, 2014.

[16] Y. Bouzelata, E. Kurt, N. Altın, and R. Chenni, "Design and simulation of a solar supplied multifunctional active power filter and a comparative study on the current-detection algorithms," *Renewable and Sustainable Energy Reviews*, vol. 43, pp. 1114–1126, 2015.

[17] F. Wang, J. L. Duarte, and M. A. M. Hendrix, "Pliant active and reactive power control for grid-interactive converters under unbalanced voltage dips," *IEEE Transactions On Power Electronics*, vol. 26, no. 5, pp. 1511–1521, 2011.

[18] A. Chaouib, J.-P. Gauberta, and F. Krima, "Power quality improvement using dpc controlled three-phase shunt active filter," *Electric Power Systems Research*, vol. 80, no. 6, pp. 657–666, 2010.

[19] Y. Suh, V. Tijeras, and T. A. Lipo, "A nonlinear control of the instantaneous power in dq synchronous frame for pwm ac/dc converter under generalized unbalanced operating condition," in *Industry Applications Society Annual Meeting (IAS), Conference Record of the IEEE*, (Pittsburgh, USA), pp. 1189–1196, October 2002.

[20] R. Cisnerosa, M. Pirroc, G. Bergnab, R. Ortegaa, G. Ippolitic, and M. Molinasd, "Global tracking passivity-based pi control of bilinear systems: Application to the interleaved boost and modular multilevel converters," *Control Engineering Practice*, vol. 43, pp. 109–119, 2015.

[21] I. L. Garciaaa, G. Espinosa-Péreza, H. Siguerdidjaneb, and A. Dòria-Cerezoc, "On the passivity-based power control of a doubly-fed induction machine," *International Journal of Electrical Power & Energy Systems*, vol. 45, no. 1, pp. 303–312, 2013.

Salem Saidi was born in Sidi Bouzid, Tunisia, in 1983. He received the M.Sc. and Ph.D degrees in electrical engineering from the Higher National Engineering School of Tunis (Ecole Nationale Supérieure d'Ingénieurs de Tunis, ENSIT), Tunis University, Tunisia, in 2009 and 2016 respectively. Dr. SAIDI is a permanent member in the Laboratory of Technologies of Information and Communication and Electrical Engineering (LaTICE). His research interests include the power electronics and machine modeling, control induction Motor drives, renewable energies, smart grid, wind turbines control, photovoltaic systems, multilevel inverter, matrix converters, reactive power control and active power filters.

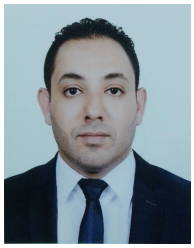

Rabeh Abbassi received his Ph.D. from the Higher National Engineering School of Tunis (ENSIT), Tunis University, Tunisia, in 2014. He was a lecturer with the Department of Electrical Engineering at ENSIT. He later joined, as an Assistant Professor, the Department of technologies at the Higher Institute of Applied Sciences and Technology of Kasserine (ISSATK) Kairouan University, Tunisia. Actually, he is an Assistant Professor at Hail University, KSA. Dr. ABBASSI is a permanent member in the Laboratory of Technologies of Information and Communication and Electrical Engineering (LaTICE). His research interests include renewable energies, smart grid, wind turbines control, photovoltaic systems, storage systems, integration of distributed generation, control of power converters, and electrical systems and power conditioning.

Nesrine Amor received her M.Sc. degree in electrical engineering from the Higher National Engineering School of Tunis (Ecole Nationale Supérieure d'Ingénieurs de Tunis, ENSIT), Tunis University, Tunisia, in 2014. Currently, she is preparing a Ph.D. degree thesis in the Laboratory of Technologies of Information and Communication and Electrical Engineering (LaTICE). Her research interests include signal processing and optimization algorithm.

Souad Chebbi received her Ph.D. from the University of Tunis, Tunisia, in 1983. She is actually a Professor with the Electrical Engineering Department of the Higher National Engineering School of Tunis (ENSIT), Tunis University, Tunisia. Dr. CHEBBI is also the head of the Laboratory of Technologies of Information and Communication and Electrical Engineering (LaTICE). Her research interests are the safety of the electrical supply networks' study and the energy management.

AUTHORS' ADDRESSES

Salem Saidi, Ph.D.
Rabeh Abbassi, Ph.D.
Nesrine Amor, M.Sc.
Prof. Souad Chebbi, Ph.D.
Department of Electrical Engineering,
Laboratory of Technologies of Information and Communication and Electrical Engineering (LaTICE),
National Higher School of Engineers of Tunis,
University of Tunis,
B.P.56-1008 Bab Menara, Tunisia.
Email: saidi_salem@ymail.com, r_abbassi@yahoo.fr, nisrine.amor@hotmail.fr, souad.chebbi@yahoo.com

Received: 2014-09-27
Accepted: 2016-03-02